# Investigation of the Deformation of Homogeneous Poly(ethylene-*co*-1-octene) by Wide- and Small-Angle X-ray Scattering Using Synchrotron Radiation

**R. ANDROSCH[1], N. STRIBECK[2], T. LÜPKE[1], S. S. FUNARI[3]**

[1] Martin-Luther-University Halle-Wittenberg, Institute of Material Science, Geusaer Str., 06217 Merseburg, Germany

[2] University of Hamburg, Institute of Technical and Macromolecular Chemistry, 20146 Hamburg, Germany

[3] Max-Planck Institute for Colloids and Interfaces, c/o HASYLAB, 22603 Hamburg, Germany

**ABSTRACT:** The deformation behavior of homogeneous ethylene-1-octene copolymers was investigated as a function of the crystallinity and the crystal size and perfection, respectively, by wide- and small-angle X-ray scattering using synchrotron radiation. The crystallinity and the crystal size and perfection, respectively, are controlled by the copolymer composition and the condition of melt crystallization. The deformation includes rotation of crystals, followed by plastic deformation and complete melting of the initial crystal population, and final formation of microfibrils. The process of rotation, plastic deformation, and melting of crystals of the initial structure is completed at lower strain if the size and perfection of the crystals, respectively, decrease, that is, if crystals thermally melt at lower temperature. The kinetics of the fibrillation of the initial structure seems independent of the crystal symmetry, that is, rotation and melting of pseudohexagonal and orthorhombic polyethylene crystals (as evident in low-crystalline specimens) are similar. The structure of the microfibrils, before and after stress release, is almost independent of the condition of prior melt crystallization, which supports the notion of complete melting of the initial crystal population. © 2002 Wiley Periodicals, Inc. J Polym Sci Part B: Polym Phys 40: 1919–1930, 2002

**Keywords:** poly(ethylene-*co*-1-octene); cold-drawing; X-ray scattering

## INTRODUCTION

The structure and properties of random, homogeneous copolymers of ethylene and 1-octene strongly depend on the composition of ethylene and 1-octene as well as the condition of crystallization. The crystallinity decreases with increasing concentration of 1-octene, and even close to completely amorphous preparations are commercialized.[1–4] The decrease of the crystallinity with increasing 1-octene concentration is paralleled by a lowering of the temperatures of primary crystallization and melting that are due to a shorter maximum length of ethylene sequences between the hexyl branches. It is assumed that the hexyl branches are excluded from the primary crystallization process that consequently results in a decrease of the thickness and perfection of crystals.[5,6] The lamellar crystal morphology of standard polyethylene with a density higher than $0.90 \text{ g cm}^{-3}$ is increasingly replaced by fringed micelles if the concentration of 1-octene increases.[7]

The crystallinity, crystal dimensions, and crystal perfection are important morphological pa-

rameters of the structure and control the macroscopic properties, including the mechanical behavior and the inherent potential of a particular copolymer for applications.[8,9] The stress at yield, the initial modulus, and the stress at break decrease, and the maximum strain increases with increasing 1-octene concentration, which is caused mainly by decreasing crystallinity.[8,10] The low-crystalline ethylene-1-octene copolymers show a stress-strain behavior that is typical for thermoplastic elastomers. The deformation behavior can be described by an advanced network theory that classifies fringed micelles and physical entanglements, respectively, as temporary and permanent network junctions, being responsible for the low permanent set after extended deformation.[8]

Uniaxial deformation of semicrystalline polyethylene includes an initial rotation and energy-elastic deformation of crystals, respectively, that is forced by the entropy-elastic/viscoelastic deformation of the surrounding amorphous structure. Plastic deformation of crystals is not assumed in the initial stage of the cold-drawing process, that is, the energy-elastic crystal deformation is reversible. Crystals orient with the chain axis parallel, perpendicular, or at an intermediate angle to the draw, respectively, depending on the shape and the local orientation within the amorphous structure. Irreversible, plastic deformation of crystals is observed when the local stress exceeds a critical value. Plastic crystal deformation can include either martensitic transformation of the orthorhombic structure into a structure of a different (internal) symmetry; fine-slip or homogeneous shear, respectively, which results in a tilt of the chain axis versus the crystal-basal plane; and coarse slip or fragmentation, respectively, that is, larger blocks are sheared to each other, without changing the angle between the chain axis and crystal-basal plane.[11–16]

The exact sequence of morphological changes during cold-drawing in this particular class of low-crystalline copolymers, however, has not been explored as opposed to the large number of investigations on standard polyethylene[11–16] and the more recent research on ethylene-1-alkene copolymers of relatively high density.[17,18] We used fast X-ray scattering techniques to monitor the change of the crystal morphology and crystal orientation, respectively, of ethylene-1-octene copolymers on uniaxial deformation. We attempt to describe the effect of the crystallinity, crystal size, and crystal perfection which are controlled by

both the copolymer composition and the thermal history, on the evolution of the deformation process. The selected copolymers exhibit a 1-octene content between 19 and 38 wt % and are well investigated with respect to the structure, crystallization, and melting behavior including annealing and stress-induced crystallization.[3,19–22]

## EXPERIMENTAL

### Material

Homogeneous metallocene-catalyzed poly(ethylene-*co*-1-octene) of different concentrations of 1-octene was provided by Dow. We determined the concentration of 1-octene by Fourier transform infrared (FTIR) spectroscopy with the integral of the absorbance between 1381 and 1373 $cm^{-1}$, which is proportional to the number of $—CH_3—$ groups.[23] Accordingly, the 1-octene content of the investigated samples was 19, 30, and 38 wt %, and the corresponding density was approximately 0.902, 0.885, and 0.870 g $cm^{-3}$, respectively. Therefore, the investigation covers specimens with a density-based crystallinity between about 15 and 35%. The melt-flow index is between 1 and 5 g $(10 \ min)^{-1}$ (463 K, 2.16 kp). Further molecular and structural information is given elsewhere[3,19–22] and in the subsequent results section. Films of 1 mm thickness were slowly cooled at a rate of 1 K $min^{-1}$ to 298 K, and films of 0.5 mm were quenched in cold water after shaping in a hydraulic press (Collin). Specimens of dimensions 100 mm length $\times$ 15 mm width were cut for the *in situ* study of the deformation behavior.

### Instrumentation

#### Calorimetry

Standard differential scanning calorimetry (DSC) was performed with a Mettler–Toledo DSC 820 with ceramic sensor FRS5. The instrument was equipped with the liquid nitrogen cooling accessory, and the furnace was purged with nitrogen at a flow rate of 80 mL $min^{-1}$. The small 20-$\mu$L aluminum pans were used for encapsulation of the samples with a mass of about 10 mg. The rate of temperature change was 20 K $min^{-1}$ on heating and 10 K $min^{-1}$ on cooling. The temperature of the sensor was calibrated using the onset of melting of indium and zinc, and the heat-flow rate was calibrated by the heat of fusion of indium.

### Density Measurements

The density of the copolymers of different branch concentrations and thermal histories was measured in a density gradient column (Ray-Ran) in a water/isopropanol mixture at 296 K. Measurements were repeated three times before averaging.

### Tensile Test

Tensile tests were done at ambient temperature with a commercial tensile-testing machine (Zwick 1425). The crosshead speed was 50 mm min$^{-1}$ with a distance between the clamps of 50 mm. The cross-section area was $4 \times 1$ mm and $4 \times 0.5$ mm for the slowly cooled and quenched samples, respectively. The stress is calculated by force per initial cross-section area, and the strain [$= (l - l_0)/l_0 \times 100\%$, where $l$ and $l_0$ are the actual and initial lengths of the sample, respectively] is monitored by position encoders with an initial distance of 20 mm.

### Wide-Angle X-ray Scattering (WAXS)

The WAXS patterns, intensity versus scattering angle $2\theta$, of isotropic samples before deformation and of relaxed samples after deformation were taken on a URD 63 diffractometer (Seifert-FPM) in the transmission mode with Ni-filtered Cu K$\alpha$ radiation (1.5418 Å). The azimuthal intensity distribution of the orthorhombic 002 reflection of the uniaxially oriented, released specimens was collected with the texture accessory TZ 6 of the diffractometer.

### Wide- and Small-Angle X-ray Scattering (WAXS and SAXS) Using Synchrotron Radiation

An *in situ* study of the deformation of the copolymers was carried out at the A2 soft-condensed matter beam line at HASYLAB at the Deutsches Elektronen Synchrotron (DESY) in Hamburg (Germany), using monochromatic radiation of a 1.5 Å wavelength. The evacuated, double-focusing camera was equipped with image plates at a distance of about 70 and 1780 mm for registration of WAXS and SAXS, respectively. The exposure time was between 10 and 20 s for registration of WAXS and 600 s for registration of SAXS, depending on the primary beam intensity. Specimens were labeled with distance marks at an increment of 2.5 mm to allow exact registration of the local deformation of the sample at the position of the beam size of about $2 \times 1$ mm using a video camera. The samples were drawn to a predefined strain, and subsequently the X-ray scattering was collected, that is, patterns were taken at constant strain. The X-ray patterns of the released samples were measured earliest, 12 h after unloading.

## RESULTS AND DISCUSSION

### Initial Structure

The initial structure of the isotropic samples before deformation was analyzed by DSC, density measurements, and WAXS. The experimental data are compactly described subsequently but are not shown to avoid repeated publication of closely connected, qualitatively similar research.

DSC heating scans revealed a decreasing final melting temperature with an increasing 1-octene content from about 374 K in the case of the sample with 19 wt % 1-octene to less than 340 K in the case of the sample with 38 wt % 1-octene. The decrease of the final melting temperature was due to a decreased maximum thickness and therefore decreased thermodynamic stability of the crystals. The maximum thickness of crystals is controlled by the maximum ethylene sequence length within the macromolecules that decreases with an increasing branch content. It is suggested that the hexyl branches are not, or are only to a limited extent, incorporated into the crystal, leading to a smaller longitudinal and lateral size of the crystals when the branch content is increased. All samples, independent of branch content and conditions of prior melt crystallization, reveal an endothermic maximum of the heat-flow rate at about 318 K because of extended annealing at ambient temperature before analysis. Isothermal annealing increases the crystallinity by no more than 3–5%, that is, annealing cannot largely affect the mechanical deformation behavior.

The density-based crystallinities of the slowly cooled and isothermally annealed samples of 1-octene concentrations of 19, 30, and 38 wt % were about 38, 25, and 15%, respectively, at ambient temperature. Crystallinity decreased in the case of the copolymer with the lowest branch content from 38 to 34% on quenching. The reduction of the crystallinity on fast cooling is expected because crystallization is kinetically controlled, that is, the nonequilibrium structure obtained by quenching freezes by sufficient lowering of the temperature as well as suppression of large-scale equilibration at ambient or subambient temperature,

respectively. The difference of the crystallinity between slowly cooled and quenched samples, however, decreases and reverses with an increasing branch content. The quenched sample with a 1-octene content of 38 wt % exhibits a slightly higher crystallinity (16%) than after slow cooling (15%), which agrees with former investigations about the effect of the cooling rate on the structure of ethylene-1-octene copolymers.[21,24]

WAXS data of the isotropic copolymers of different branch contents and different thermal histories confirm the increasing crystallinity on decreasing branch content and show a distinct influence of the thermal history on the X-ray structure. The intensity of the orthorhombic reflections apparently decreases with an increasing cooling rate during melt crystallization, which points to less orthorhombic crystallinity and/or less-ordered/smaller orthorhombic crystals, respectively. Additionally, we observed a decrease of the density of the orthorhombic phase that is indicated by the shift of the 110 and 200 reflections. Furthermore, we need to point to an additional scattering intensity at about 4.5 Å in the case of the quenched sample with a 1-octene content of 38 wt % caused by a pseudohexagonal structure that increasingly develops when increasing the cooling rate on melt crystallization.[19,20,25]

## Tensile Testing

Figure 1 depicts the stress-strain curves of slowly cooled (thin line) and quenched (thick line) poly-(ethylene-*co*-1-octene) of different branch contents. The initial modulus and stress at yield increase with increasing crystallinity and a decreasing branch content, respectively. The stress reaches a plateau subsequent to the yield point; both are most distinctly observed in the sample of high crystallinity. The following increase of stress, that is, strain hardening, can be attributed to a tightening of the entanglement network of the amorphous phase or stress-induced crystallization, respectively. The low-crystalline specimen does not suggest a clear yield point but an immediate decrease of the modulus at small strain, that is, the deformation of the low-crystalline copolymer appears to be largely controlled by the amorphous phase. Nonetheless, we have observed pronounced stress-induced crystallization of the low-crystalline sample in previous investigations,[20,22] which can explain the increase of stress at large deformation. The insert is an enlarge-
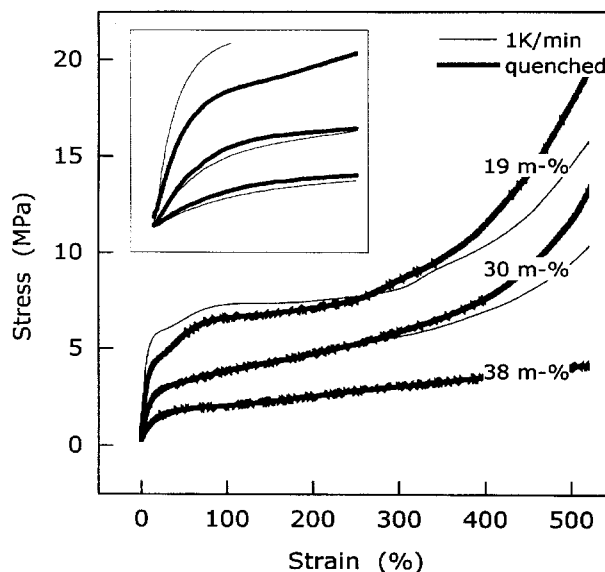


**Figure 1.** Stress-strain curves of slowly cooled and quenched poly(ethylene-*co*-1-octene) with 19, 30, and 38 wt % 1-octene.

ment of the stress-strain curves during the initial stage of the deformation and reveals the influence of thermal history on the macroscopic deformation behavior. The initial modulus and stress at yield are directly related to the crystallinity. The low-crystalline specimen shows after quenching a slightly higher crystallinity than after slow cooling, and, consequently, the modulus and stress at yield of the quenched sample increase. The situation is reversed in the case of the relatively high-crystalline specimen that contains 19 wt % 1-octene. The influence of the thermal history on the (viscoelastic) deformation behavior is confirmed by a separate in-depth study of the effect of the morphology of ethylene-1-octene copolymers on the mechanical relaxation behavior.[26]

### *In situ* Study of the Deformation by WAXS and SAXS

#### *Poly(ethylene-co-1-octene) with 19 wt % 1-Octene*

Figure 2 shows the equatorial WAXS in the angular region of the 110 and 200 reflections (left) and SAXS (right) of slowly cooled poly(ethylene-*co*-1-octene) with concentration on 1-octene of 19 wt % as a function of strain, recorded on a quasi-continuous drawing. Figure 3 illustrates the X-ray pattern of a quenched specimen of identical molecular composition. The draw direction is ver-
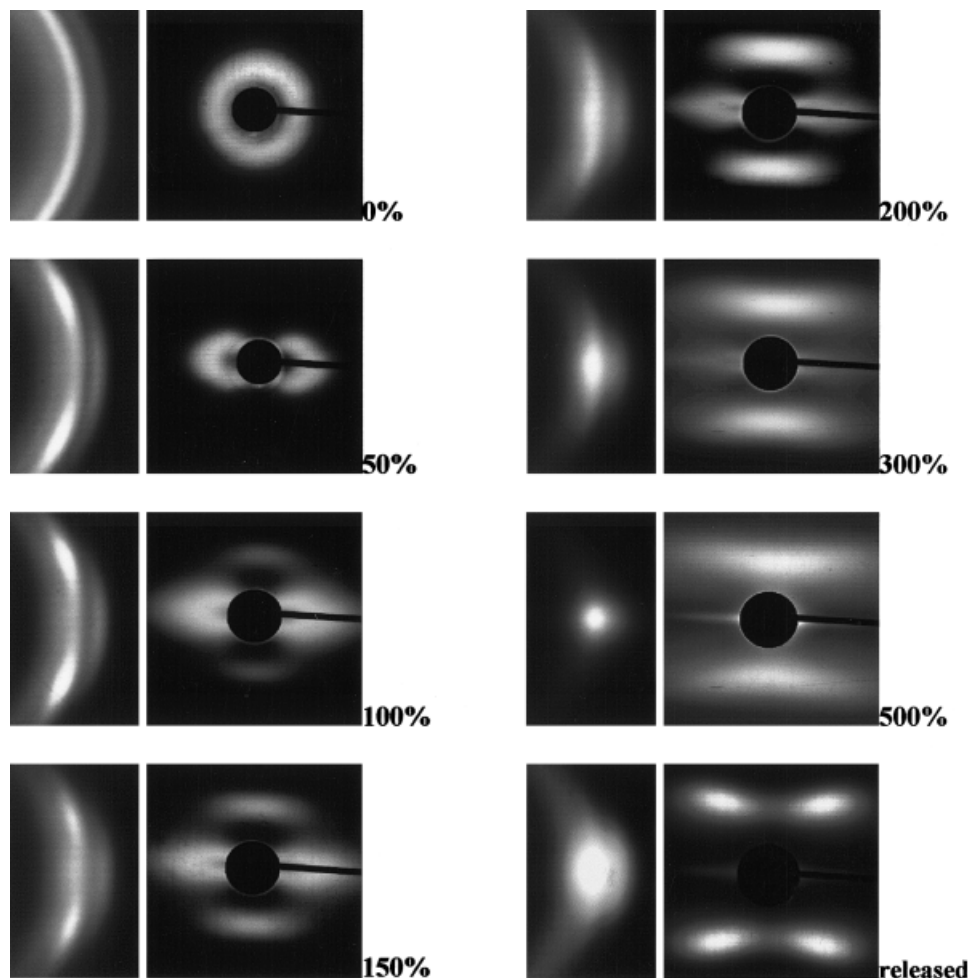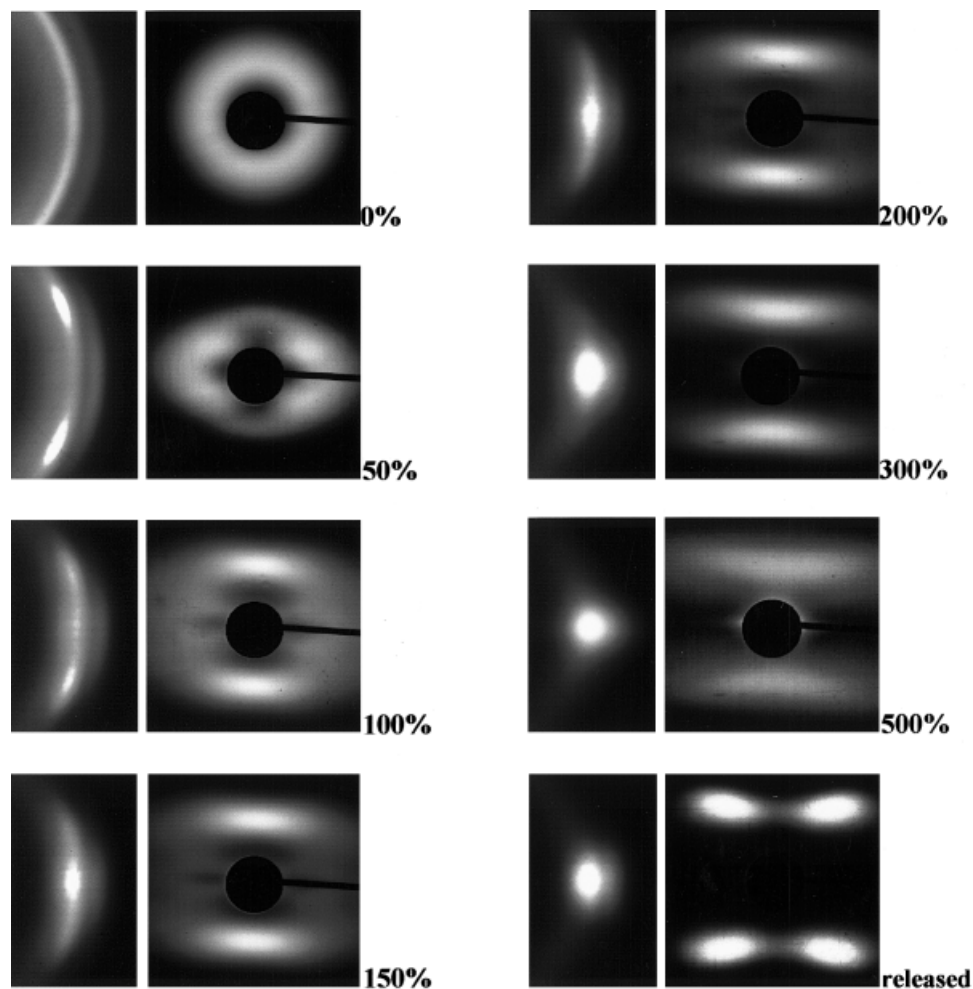
**Figure 2.** Equatorial WAXS in the angular region of the 110 and 200 reflections (left) and SAXS (right) of slowly cooled poly(ethylene-*co*-1-octene) with 19 wt % 1-octene as a function of strain. The draw direction is vertical.

tical. The long period after cooling from the melt at a rate of 1 K min$^{-1}$ is about 197 Å and decreases as a result of quenching to about 156 Å. Figure 4 is a plot of the meridional and equatorial long periods of both preparations as a function of strain. SAXS of the slowly cooled sample shows at small strain (50%) a "figure-eight pattern" that is due to a superposition of four radial dashes and two arcs. The angle between the equator and the tangent of the radial dashes decreases with increasing distance from the center of the pattern, and the two equatorial spots are located at a distance of about 172 Å. Figure-eight patterns can be explained by a structure that simultaneously contains stacks of lamellae that are oriented perpendicular to the draw direction, causing the equatorial maximum and tilted lamellae as well as the off-equatorial dashes/arcs.[27] The direction

of the normal of the tilted lamellae is along the dashes/arcs and can probably adopt any angle between 90° (meridian, in beam stop) and 0° (equator) at varying distance. The different orientation of the lamellae results from the initial shape and orientation to the draw, that is, it is the result of the local stress at the respective lamellae.

The equatorial intensity maximum observed at medium strain is still assigned to a stacking of lamellae originating from the initial structure. The decreased long period can be explained by lateral compression of the stack that is caused by the applied uniaxial stress. The figure-eight pattern as a whole is observed up to 300% strain, and the angle between the equator and the radial dashes is reduced with increasing strain, respectively. The intensity of this pattern gets weaker

**Figure 3.** Equatorial WAXS in the angular region of the 110 and 200 reflections (left) and SAXS (right) of quenched poly(ethylene-*co*-1-octene) with 19 wt % 1-octene as a function of strain. The draw direction is vertical.

on expense of the meridional scattering that is observed first at a strain of 100% at a distance of about 137 Å. The meridional long spacing is almost unchanged in distance on further drawing; its shape, however, develops into a distinct streak parallel to the equator, indicative for the formation of microfibrils. WAXS at 50% strain is described by a four-point pattern of the 110 reflection with maxima located at an angle of 22° off the equator, decreasing on further drawing. The 110 reflection exhibits a six-point pattern by additional appearance of an equatorial peak at 150 and 200% strain, which points to two coexisting crystal populations. The 200 reflection, in turn, is located at the equator from the very beginning of the deformation. After drawing the sample to 500% strain, the sample was released from the stress. The strain reverts to about 360%, which is

paralleled by a decrease of the crystal orientation. The sloped four-point SAXS pattern reveals tilt of the basal plane of crystals within the microfibrils.

The SAXS figure-eight pattern has been explained by rotation of stacks of lamellae originally oriented at random. The distance between lamellae depends on the orientation to the draw and is adjusted by interlamellar slip. The WAXS pattern reveals that at all draw ratios the most probable *a*-axis orientation is exactly perpendicular to the draw direction. At low strain, the *c* axis (chain direction) is oriented at some intermediate angle between the equator and the meridian, as can be concluded from the split, nonequatorial maxima of the 110 reflection. Subsequently, on increasing strain, the 110 reflection moves toward the meridian. The off-equatorial 110 reflection appears to be associated with the observation of the fig-
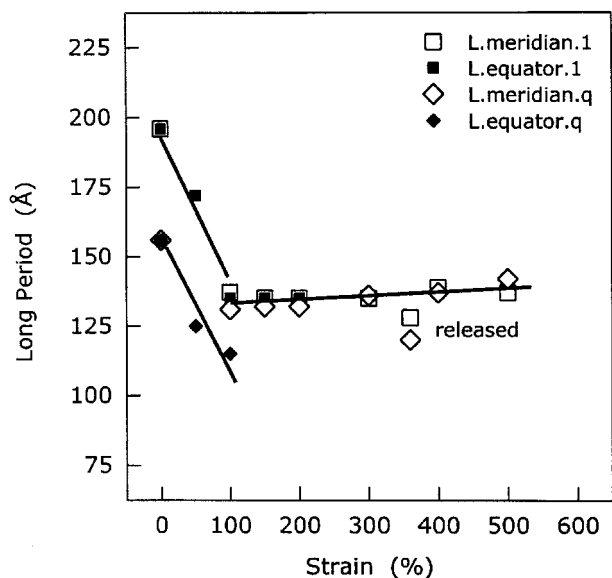
**Figure 4.** Meridional and equatorial long period of slowly cooled and quenched poly(ethylene-*co*-1-octene) with 19 wt % 1-octene as a function of strain.

ure-eight SAXS pattern. However, a quantitative comparison of stack orientation and crystal orientation, to detect the tilt of the chain axis respective to the surface of the lamella (fine slip),[28] is impossible because of the arclike character of the SAXS intensity, that is, we cannot extract a single orientation of stacks and the corresponding crystal orientation. The merging 110 peak seems to be correlated to the SAXS meridional layer-line pattern at large strain and reflects a second crystal population, likely formed as a result of fibrillation of initial, rotated, and plastic deformed lamellae. The SAXS pattern of the released sample shows intensity maxima at an angle of about 35° off the meridian with the sloped dashlike maxima elongated toward the radius, pointing to considerable tilt of the crystal basal plane while keeping the chain direction parallel to the former draw direction. The tilt of microcrystals within the fibril must be due to longitudinal shear in the chain direction that is transferred by interfibrillar tie-molecules, originating from neighboring, sliding fibrils.[29]

The WAXS and SAXS patterns of the quenched specimen are displayed in Figure 3 as a function of strain. Qualitatively, the patterns look similar to the corresponding patterns of the slowly cooled sample (Fig. 2). SAXS indicates at low strain an elliptical pattern with the long axis in the equatorial direction, superimposed by four distinct maxima at an angle of about 25° off the equator

and at a distance of about 155 Å. The long period of 156 Å of the isotropic sample reduces in the equatorial direction to about 125 Å because of the compression of stacks of lamellae oriented perpendicular to the draw and does not show significant changes in the meridional direction. The figure-eight pattern, which develops at low and intermediate strain, is much less pronounced than in the case of the slowly cooled sample. An obvious explanation for this observation is the lower perfection of the crystalline lamellae and their stacking in the quenched material. Moreover, this notion also explains the appearance of the SAXS layer-line pattern at lower strain than in the case of the slowly cooled specimen because a less perfect lamellar nanostructure can be transformed more easily into the microfibrillar structure. The transformation of considerable fractions of lamellae into microfibrils, again, goes along with the observation of the 110 reflection centered about the equator. At a strain of 100% the remaining lamellar structure is still detected by a distinct six-point pattern of the 110 reflection. Figure 5 demonstrates the azimuthal intensity distribution of quenched and slowly cooled poly(ethylene-*co*-1-octene) as a function of strain up to 200%. The off-equatorial peaks shift on increasing strain toward the equator at 180°; how-
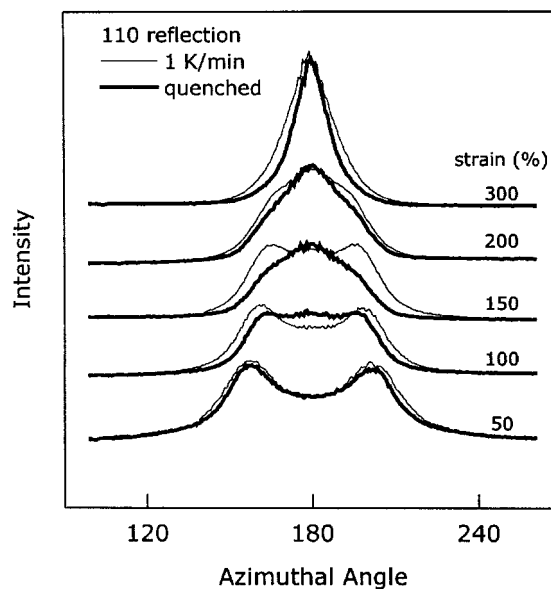


**Figure 5.** Azimuthal intensity distribution of the WAXS 110 reflection of quenched and slowly cooled poly(ethylene-*co*-1-octene) with 19 wt % 1-octene as a function of strain between 0 and 300%. The equator is at 180°.
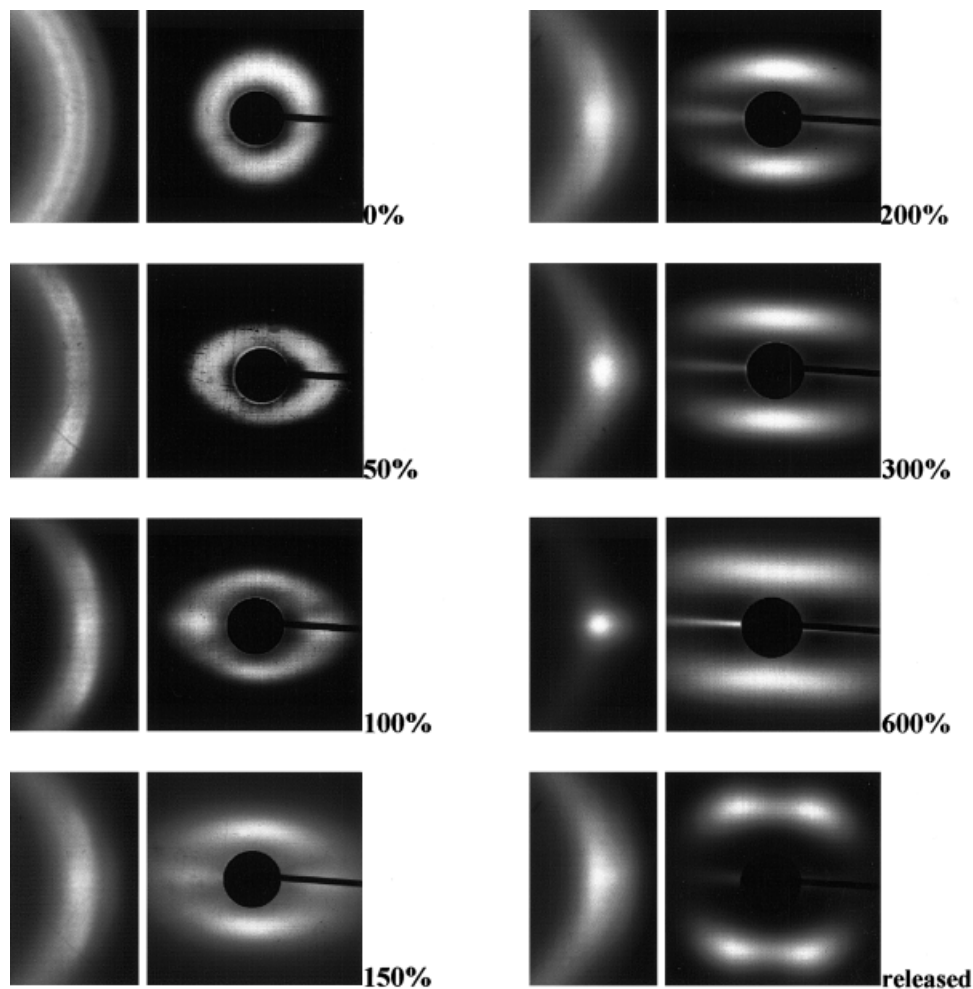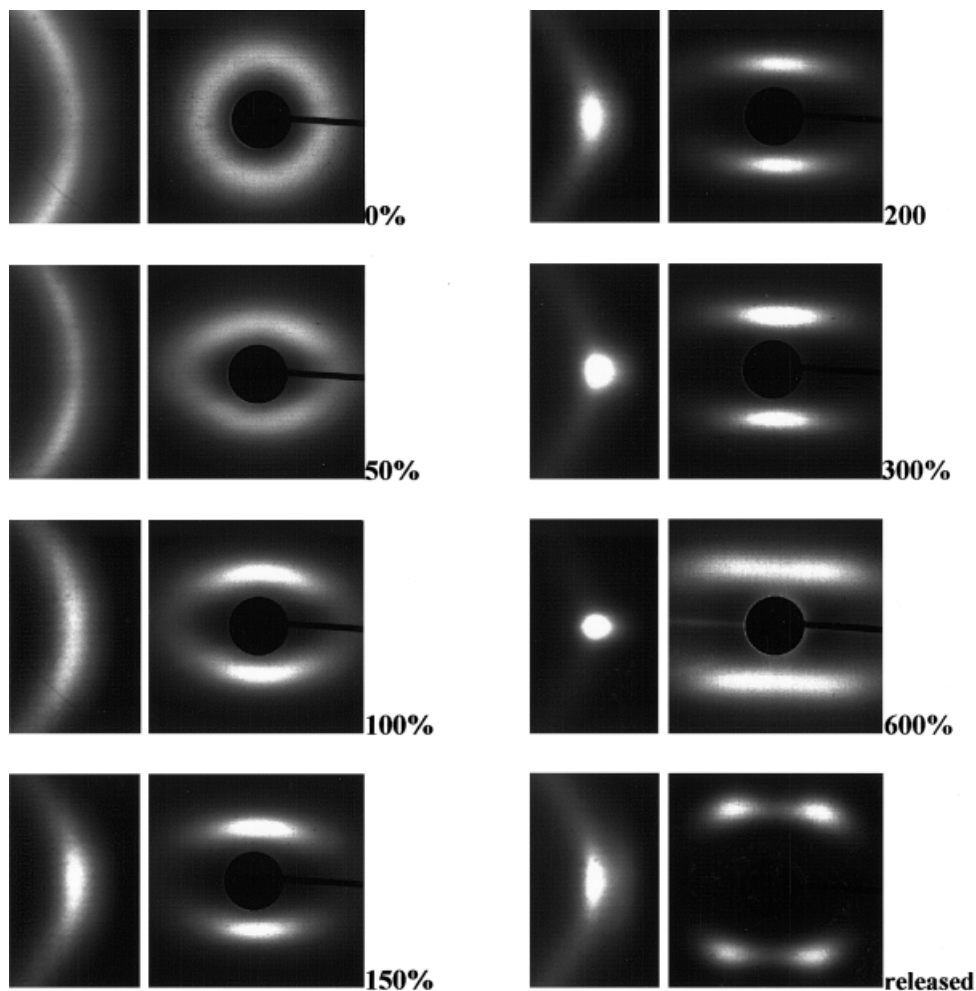
**Figure 6.** Equatorial WAXS in the angular region of the 100 pseudohexagonal and 110/200 orthorhombic reflections (left) and SAXS (right) of slowly cooled poly(ethylene-*co*-1-octene) with 38 wt % 1-octene as a function of strain. The draw direction is vertical.

ever, the equatorial peak, which likely represents the micro-fibril-crystal fraction, is seen with a discrete maximum already at 100% strain in the case of the quenched sample, in contrast to 150% strain in the case of the slowly cooled sample. The radial half-width of the 110 and 200 reflections simultaneously increase considerably because of the limited lateral crystal size, apparently merging into one single reflection at a high draw ratio.

### Poly(ethylene-co-1-octene) with 38 wt % 1-Octene

Figures 6 and 7 describe the equatorial WAXS and SAXS patterns of slowly cooled and quenched poly(ethylene-*co*-1-octene) with 38 wt % 1-octene, respectively; Figure 8 is a plot of the equatorial and meridional SAXS long period of both prepa-

rations as a function of strain. The initial structure is characterized by the coexistence of an orthorhombic crystalline phase, a pseudohexagonal mesophase, and the amorphous phase. The pseudohexagonal structure is not seen in the sample with 19 wt % 1-octene and seems typical for poly(ethylene-*co*-1-octene) of high comonomer concentration. In the case of the isotropic and undrawn sample, the mesophase can hardly be distinguished from the amorphous halo in the WAXS pattern because of the close correspondence of the maximum position. The two isotropic Debye–Scherrer rings at zero draw ratio are the amorphous halo/100-mesophase maximum at a distance of about 4.5 Å and the 110 orthorhombic reflection at a distance of 4.22 Å. Drawing by 50% results in rotation of both, orthorhombic and

**Figure 7.** Equatorial WAXS in the angular region of the 100 pseudohexagonal and 110/200 orthorhombic reflections (left) and SAXS (right) of quenched poly(ethylene-*co*-1-octene) with 38 wt % 1-octene as a function of strain. The draw direction is vertical.

pseudohexagonal crystals enable clear differentiation of the mesomorphic and amorphous structure. The 100 pseudohexagonal and 110 orthorhombic reflections appear at 22° off the equator, similar to poly(ethylene-*co*-1-octene) with 19 wt % 1-octene. Obviously, the internal symmetry of the orthorhombic and pseudohexagonal structure, respectively, is irrelevant for the initial crystal rotation unlike the overall morphology and shape of crystals and force transmission by tie-molecules into the crystal. Otherwise, we hardly would have obtained the 100 pseudohexagonal and 110 orthorhombic peaks at the same azimuth. Furthermore, the patterns do not provide any indication for a stress-induced transformation from the orthorhombic structure to the monoclinic structure.[30–32] The SAXS pattern of the isotropic sample suggests a long period of about 165–170 Å.

The long period decreases to about 130 Å in the equatorial direction at 100% strain. At the meridian we can see a continuous transition of the ellipsoidal scattering at 50% strain to an arc between 100 and 200% strain, which finally develops into a streak at a strain larger than 300%. Simultaneously, we detect continuous azimuthal merging and radial broadening as a result of the decreasing lateral crystal size of the off-equatorial 100 mesophase and 110 orthorhombic reflections that seem almost complete at about 200% strain. The evolution of the meridional arc in SAXS at 100% strain goes along with the appearance of equatorial peaks of the 100 mesophase and 110 orthorhombic reflections, that is, the four-point pattern of both reflections transfers into a six-point pattern, pointing also in this low-crystalline copolymer to coexisting and differently
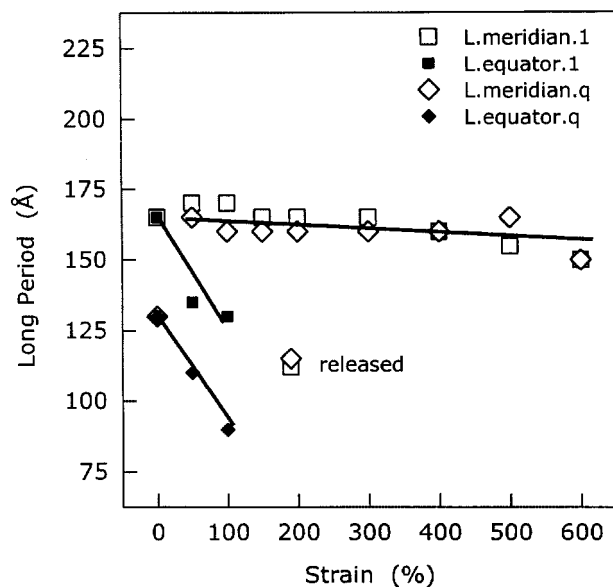
**Figure 8.** Meridional and equatorial long period of slowly cooled and quenched poly(ethylene-*co*-1-octene) with 38 wt % 1-octene as a function of strain.

oriented crystal populations. Between 100 and 200% strain, we see coexisting stacks of lamellae/ microcrystals that are oriented perpendicular and parallel to the draw. At 300% strain, the fraction of initial lamellae disappeared, and only the fibrillar structure of perfectly oriented and stacked microcrystals and the amorphous phase remains. The released sample exhibits a permanent set of about 190%, after drawing to 700% of the initial length. The recovery is accompanied by a decrease of the WAXS degree of orientation and tilt of the basal plane of the microcrystals within the fibrils.

The quenched specimen with 38 wt % 1-octene shows in the isotropic state a single broad maximum in the WAXS pattern that can hardly be indexed because it might contain intensity contributions of both the mesomorphic and orthorhombic structures. Small strain results in a four-point WAXS pattern, with the azimuthal maxima merging at the equator at 150% strain. We cannot resolve a six-point pattern because of the broadness of the peaks; however, the absence of discrete equatorial SAXS maxima points to early destruction of relatively unstable crystals. Despite the absence of distinct equatorial maxima, as we have seen in the SAXS pattern of the slowly cooled sample, the equatorial long period, estimated from the ellipsoid, decreases like the slowly cooled sample, pointing to qualitatively

similar deformation mechanisms (Fig. 8). SAXS reveals a meridional arc at low strain that continuously transforms to a well-developed streak at a strain higher than 300%. The layer-line distance is about 160 Å and is almost independent of strain (Fig. 8).

### Poly(ethylene-co-1-octene) with 30 wt % 1-Octene

The X-ray patterns of the copolymer with 30 wt % 1-octene are not shown but are described in detail because the sequence of the structural changes on deformation is similar to the copolymers with 19 and 38 wt % 1-octene. The long period of the nondrawn sample is in sequence with the long period of the copolymers with 19 and 38 wt % 1-octene, that is, the initial long period decreases for both the slowly cooled and quenched preparations, with an increasing 1-octene content (Fig. 9). The quenched sample again indicates a decreased long period if compared with the long period of the slowly cooled sample. The initial crystal population is detected up to about 100–200% strain for the quenched and slowly cooled sample, respectively. The meridional long period is around 150 Å and is in this case independent of the thermal history.

### Structure of Released Specimens

The WAXS 002 reflection of drawn and subsequently relaxed samples is exactly positioned at
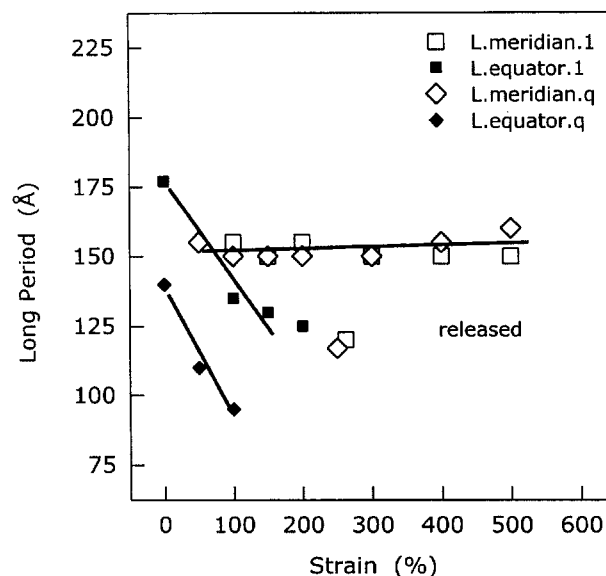


**Figure 9.** Meridional and equatorial long period of slowly cooled and quenched poly(ethylene-*co*-1-octene) with 30 wt % 1-octene as a function of strain.

the meridian, although broadened and exhibiting a half-width of about 27°, but not showing any indication of off-meridional maxima. The SAXS four-point pattern shows the maxima at about 30–35° off the meridian, clearly proving their origin from tilted basal planes of crystals rather than tilted fibrils/chains. The layer-line distance of about 115–125 Å is almost independent of the copolymer composition, and the off-meridional angle is approximately identical for all investigated copolymers. However, both the maximum strain and the permanent set of the samples of different comonomer contents are different. The permanent set increases, as expected, with decreasing 1-octene concentration. The SAXS pattern of the released samples exhibit largely identical symmetry and distance despite large differences of the chemical structure, that is, branch concentration, and initial structure including crystal thickness/shape and crystallinity. The only obvious difference of the SAXS pattern of the relaxed samples is the shape of the maxima, pointing to a different shape of the microfibrillar crystals. The intensity maxima of the specimen with a low comonomer content (Figs. 2 and 3) are elongated in the radial direction, whereas in the case of the specimen of a higher comonomer content (Figs. 6 and 7), the maxima are pointlike.

## FINAL DISCUSSION AND CONCLUSIONS

The deformation of homogeneous poly(ethylene-*co*-1-octene), as probed by X-ray techniques, resembles the deformation of low-density standard polyethylene, that is, the type and sequence of characteristic scattering patterns are similar as observed in previous investigations.[15] The deformation includes rotation and slip of crystals followed by formation of fibrils. We have found no evidence for a transition from the orthorhombic to the monoclinic structure as has been occasionally reported.[16–18,30–32] The kinetics of the deformation-induced structural changes depends on the concentration on 1-octene and the thermal history because both affect systematically the initial morphology of the copolymers, including the crystallinity and dimension/perfection of the crystals. The increase of the comonomer concentration from 19 to 38 wt % shifts the process of melting/destruction of the initial crystal population and the formation of microfibrils, respectively, to lower strain. A lower activation energy for plastic deformation of the initial crystal population is apparently required if crystals thermally melt at a lower temperature, that is, if crystals are smaller and contain more defects. The new population of crystals, which is oriented with the chain axis parallel to the draw, can form at lower strain if the initial crystals are removed and the orientation of amorphous structure is not restricted by remaining crystals. The formation of microfibrils at lower strain in the case of the copolymer with 38 wt % 1-octene, remarkably, is paralleled by an increased inherent potential for stress-induced crystallization as compared with the copolymer with only 19 wt % 1-octene. A previous study about the irreversible and reversible crystallization behavior of the particular low-crystalline ethylene-1-octene copolymer revealed stress-induced crystallization from the beginning of deformation, mainly including material that would have crystallized at subambient temperatures.[22] The copolymer with 19 wt % 1-octene does not contain the required short ethylene sequences that would thermally crystallize at ambient or subambient temperature, respectively, and this might cause the higher activation energy for the onset of microfibril formation.

Quenched specimens exhibit smaller crystals in both the longitudinal and lateral directions.[33] The decrease of the longitudinal crystal dimension in quenched samples was indirectly detected by SAXS, and the broadening of the equatorial WAXS confirms the effect of quenching on the lateral crystal size. Because there is only a minor effect of the crystallization history on the total crystallinity, the deformation behavior must be changed because of the altered crystal morphology. The X-ray data of this study clearly suggest that smaller crystals require lower critical strain for destruction than larger crystals, as is easily derived from a direct comparison of the X-ray pattern, for example, taken at 150% strain.

The distance between crystals within the microfibrils in the final stage of the deformation is largely independent of both the branch content and the thermal history. This result leads to the conclusion of complete reorganization of the initial structure, including melting of crystals that were formed on melt crystallization, on deformation. Further evidence for this conclusion is provided by analysis of the structure after stress release; the macroscopic permanent set and structure of microfibrils, respectively, depend on the copolymer composition but are not affected by the thermal history. The dependence of the structure of stress-released samples on the chemical com-

position is the consequence of the largely different crystallinity, that is, the number of temporary and permanent network junctions.

## REFERENCES AND NOTES

1. Alizadeh, A.; Richardson, L.; Xu, J.; McCartney, S.; Marand, H.; Cheung, Y. W.; Chum, S. Macromolecules 1999, 32, 6221.
2. Schulze, U.; Arndt, M.; Freidanck, F.; Beulich, I.; Pompe, G.; Meyer, E.; Jehnichen, D.; Pionteck, J.; Kaminsky, W. J Macromol Sci Pure Appl Chem 1998, A35, 1037.
3. Androsch, R.; Wunderlich, B. Macromolecules 1999, 32, 7238.
4. Product information Engage Polyolefin Elastomer, DuPont Dow Elastomer, Sept 2001.
5. Mathot, V. B. F.; Scherrenberg, R. L.; Pijpers, T. F. J.; Engelen, Y. M. T. Structure, Crystallization and Morphology of Homogeneous Ethylene-Propylene, Ethylene-1-Butene and Ethylene-1-Octene Copolymers with High Comonomer Contents. In New Trends in Polyolefin Science and Technology; Hosoda, S., Ed.; Research Signpost: Trivandrum, India, 1996; p 71.
6. Mathot, V. B. F.; Scherrenberg, R. L.; Pijpers, T. F. J. Polymer 1998, 39, 4541.
7. Bensason, S.; Minick, J.; Moet, A.; Chum, S.; Hiltner, A.; Baer, E. J Polym Sci Part B: Polym Phys 1996, 34, 1301.
8. Bensason, S.; Stepanov, E. V.; Chum, S.; Hiltner, A.; Baer, E. Macromolecules 1997, 30, 2436.
9. Sehanobish, K.; Patel, R. M.; Croft, B. A.; Chum, S. P.; Kao, C. I. J Appl Polym Sci 1994, 51, 887.
10. Kennedy, M. A.; Peacock, A. J.; Failla, M. D.; Lucas, J. C.; Mandelkern, L. Macromolecules 1995, 28, 1407.
11. Peterlin, A. J Polym Sci Part C: Polym Symp 1966, 15, 427.
12. Peterlin, A. J Polym Sci Part C: Polym Symp 1967, 18, 123.
13. Meinel, G.; Morosoff, N.; Peterlin, A. J Polym Sci Part A-2: Polym Phys 1970, 8, 1723.
14. Bowden, P. B.; Young, R. J. J Mater Sci 1974, 9, 2034.
15. Peterlin, A.; Balta-Calleja, F. J. Kolloid Z Z Polym 1970, 242, 1093.
16. Butler, M. F.; Donald, A. M.; Bras, W.; Mant, G. R.; Derbyshire, G. E.; Ryan, A. J. Macromolecules 1995, 28, 6383.
17. Butler, M. F.; Donald, A. M.; Ryan, A. J. Polymer 1997, 22, 5521.
18. Butler, M. F.; Donald, A. M. Macromolecules 1998, 31, 6234.
19. Androsch, R. Polymer 1999, 40, 2805.
20. Androsch, R.; Blackwell, J.; Chvalun, S. N.; Wunderlich, B. Macromolecules 1999, 32, 3735.
21. Androsch, R.; Wunderlich, B. Macromolecules 2000, 33, 9076.
22. Androsch, R.; Wunderlich, B.; Lüpke, T.; Wutzler, A. J Polym Sci Part B: Polym Phys, 2002, 40, 1223.
23. Pump, W.; Woltjes, D. Kunstst 1979, 69, 317.
24. Peeters, M.; Goderis, B.; Reynaers, H.; Mathot, V. J Polym Sci Part B: Polym Phys 1999, 37, 83.
25. Peeters, M.; Goderis, B.; Vonk, C.; Reynaers, H.; Mathot, V. J Polym Sci Part B: Polym Phys 1997, 35, 2689.
26. Kolesov, I.; Androsch, R.; Radusch, H.-J. Bulletin APS Meeting, Indianapolis, March 18–22, 2002, American Institute of Physics, Vol. 47, No. I, Part II, p 846.
27. Gerasimov, V. I.; Genin, Y. V.; Tsvankin, D. Y. J Polym Sci Polym Phys Ed 1974, 12, 2035.
28. Peterlin, A.; Meinel, G. Makromol Chem 1971, 142, 227.
29. Meinel, G.; Peterlin, A. Eur Polym J 1971, 7, 657.
30. Seto, T.; Hara, T.; Tanaka, K. Jpn J Appl Phys 1968, 7, 31.
31. Bevis, M.; Crellin, E. B. Polymer 1971, 12, 666.
32. Russell, K. E.; Hunter, B. K.; Heyding, R. D. Polymer 1997, 38, 1409.
33. Wunderlich, B. Crystal Nucleation, Growth, Annealing. In Macromolecular Physics; Academic: New York, 1976; Vol. 2, Chapter 5.1, pp 1–72.